Heliyon 9 (2023) e19142

Contents lists available at ScienceDirect

Heliyon

journal homepage: www.cell.com/heliyon

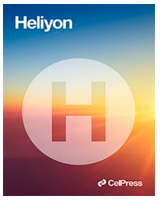

Review article

Systematic literature review of cold-formed steel at elevated temperature scenario☆

Cheryl Lyne C. Roxas [a], Carluz R. Bautista [b], Orlean G. Dela Cruz [c], Rhem Leoric C. Dela Cruz [d], John Paul Q. De Pedro [d,*], Jonathan R. Dungca [a], Bernardo A. Lejano [a], Jason Maximino C. Ongpeng [a]

[a] *Faculty, Department of Civil Engineering and Center for Engineering and Sustainable Development Research, De La Salle University, Philippines*
[b] *Science Research Specialist, Philippine Council for Industry, Energy and Emerging Technology Research and Development, Philippines*
[c] *Faculty, Polytechnic University of the Philippines, Philippines*
[d] *Research Assistant, Center for Engineering and Sustainable Development Research, De La Salle University, Philippines*

ARTICLE INFO

Keywords:
Cold-formed steel
Light gauge steel
Systematic literature review
Elevated temperature
High temperature
Finite element analysis
Experimental methods
Fire performance
Screw connections

ABSTRACT

Cold-formed steels (CFS) or light gauge steels (LGS) are steel sections created through processes without heat application, such as roll forming or press-braking. In the past few decades, the utilization of CFS as a structural material has expanded due to its advantages over the other materials used in the construction industry, consequently increasing the number of studies conducted by many researchers. CFS studies have focused on many research areas, including designing, and analyzing members and systems, connections, sustainability, residual stresses, and post-fire data. As a result, several authors have also conducted a literature review involving these areas. However, a literature review for more recent studies involving elevated temperature exposure of CFS has not been conducted. This paper seeks to compile and review the recent publications regarding CFS behavior and performance at high temperatures events. Sixty-nine (69) journal articles published from 2017 to 2023 were retrieved from the Scopus database and systematically reviewed through text mining with the aid of VOS Viewer. Prior studies utilizing finite element analysis and experimental methods to investigate the performance at elevated temperature events of varying CFS sections, systems, and steel grades have been summarized. In addition, this paper also briefly discussed the findings of the recent research works involving member connections of CFS. Key points from the literature review have been emphasized such as the outcome of experimental and numerical validation of existing design rules from different codes such as American Iron and Steel Institute (AISI), Eurocodes, and Australian codes which could vary depending on the CFS section and steel grades. Important points of previous studies regarding the CFS walls, insulations, and screwed connections have also been noted in this paper. Based on the review, research gaps in the prior studies involving elevated temperature exposure of CFS have been identified, such as lack of CFS investigation under fatigue and cyclic

☆ Cheryl Lyne C. Roxas reports financial support for the research project involving this paper was provided by Republic of the Philippines Department of Science and Technology (DOST) through the Science for Change Program (S4CP) – Collaborative Research and Development to Leverage Philippine Economy (CRADLE). Cheryl Lyne C. Roxas reports administrative support was provided by DOST Philippine Council for Industry, Energy, and Emerging Technology Research and Development (PCIEERD) as the monitoring agency of the research project involving this paper.

* Corresponding author. Research Assistant, Center for Engineering and Sustainable Development Research, De La Salle University, Philippines.
E-mail address: john.paul.depedro@dlsu.edu.ph (J.P.Q. De Pedro).

https://doi.org/10.1016/j.heliyon.2023.e19142
Received 20 December 2022; Received in revised form 8 March 2023; Accepted 14 August 2023
Available online 14 August 2023

loading. These were then recommended as future direction and concentration of CFS at elevated temperatures research works.

1. Introduction

Cold-formed steels (CFS) or light gauge steels (LGS) are steel sections manufactured at ambient temperature [1]. The sections, typically thin-walled, are crafted either by stamping or pressing thin gauge steel sheets into the appropriate cross-section [2] or by rolling steel coil or strip through a number of rollers that gradually form the design profile without the usage of heat treatment [3]. CFS was first used in building construction in England and the United States in the 1850s [4]. Over the past few decades, the application of CFS has grown, beginning with its application in housing systems, one-story sheds, secondary support structures, and frame structures [5]. The rise in demand for using the CFS in structures, particularly in light constructions, was brought upon by the benefits that it offers as a building material: lightweight, high capacity, ease of prefabrication, improvement in assembly, more detailing accuracy, consistent quality, the cost efficiency in handling and transportation, noncombustible, and recyclable [6]. These advantages posed by the usage of CFS over other construction materials have caused a rapid escalation of its use, and in the research aspect, specifically in industrialized countries like the United States of America, Canada, China, Australia, and other European countries [7].

With the CFS research field expanding quickly, several authors have done several literature reviews of earlier studies on CFS. Gregory J. Hancock has conducted a review article for major research done over 1999–2001 as issued in reputable publications on thin-walled steel structures [8]. The same author published another review article for CFS research over the years 2013–2014, where his review is limited to articles from three journals: Journal of Constructional Steel Research, Thin-Walled Structures, and the Journal of Structural Engineering, and added conference papers from significant conferences transpired at the time: the 22nd International Specialty Conference on Cold-Formed Steel Structures (St. Louis, MO, USA), the 7th International Conference on Thin-Walled Structures (Busan, Korea) and the Eurosteel 2014 (Naples, Italy) [3]. When it comes to CFS connections, Lee et al. reviewed earlier studies that concentrated on bolted, welded, storage rack, and screwed connections, and their performance [9]. Authors like Ananthi focused on examining the research on the CFS channel sections that are axially and eccentrically compressed [10]. Regarding CFS beams and column characteristics at elevated temperatures, Javed et al. extensively reviewed the experimental and numerical studies involving these components [11]. Additionally, Yu et al. gave an extensive literature evaluation for studies that discussed cold-formed and hot-rolled steel data after being subjected to fire [12]. The review by Diaz et al. covered methods used in previous studies—both computationally and experimentally—to assess residual stresses in CFS members [13]. More recently, Liang et al. reviewed the prior studies on the CFS structures' thermal performance and the optimization of CFS structural sections [14].

For previous studies about CFS systems, Sani et al. provided a review on roof trusses constructed using CFS [15], and Sharafi et al. focused on the research and advancements made in the lateral resistance of lightweight steel frames [16]. In addition, Di Lorenzo and De Martino provided an outline of the CFS non-structural architectural and structural systems' existing codification and ongoing research [17]. Other authors like Amsyar et al. gathered and reviewed prior studies on composite joints for CFS structures, focusing on three distinctive topics: composite beam-to-column and beam-to-slab joints, and beam-to-column joints [18]. Usefi et al. examined and summarized the key numerical research advancements on the lateral performance of CFS framed shear wall constructions [19].

The properties, analysis, and design of CFS components and systems have received more attention in recent literature studies written by other authors. However, the latest studies on high-temperature properties and behaviors of CFS were not reviewed extensively. Due to exposure to higher temperatures during incidents of fire, the steel sections' mechanical properties rapidly decline. This phenomenon significantly reduces steel section load-carrying capability [20]. As such, knowledge regarding CFS characteristics and performance at elevated temperature scenarios is essential for proper structural design considering fire or evaluating the degree of damage caused by fire and their potential reuse with or without the necessity of retrofitting. In this paper, the recent research works conducted in the last five years (2017–2022) for the elevated temperature CFS properties and behavior were systematically collected and reviewed through text mining methods using the software VOS Viewer. The systematic review's objective was to present a summary of recent research conducted on CFS, specifically information on its elevated temperature characteristics. Additionally, this study recognized the research gaps and potential future studies for the increased temperature properties of CFS.

Table 1
Results of CFS at elevated temperature literature retrieval and selection.

Databases	Scopus	Initial Records: 9409Documents
Logical Statement	"cold AND formed AND steel" OR "light AND gauge AND steel" AND "elevated AND temperature"	Valid records for First Round filter: 290 Documents
Inclusion Criteria	a. Year: 2017, 2018, 2019, 2020, 2021, 2022, 2023 b. Subject Area: Engineering c. Document Type: Article d. Source Type: Journal e. Language: English	Valid records for Second Round Filter: 98 Documents

2. Methodology

2.1. Literature gathering using the scopus database

Using the sophisticated retrieval feature in the Scopus database, papers relating to CFS published between 2017 and 2023 were located; the screening procedure is displayed in Table 1 for elevated temperature topics. To ensure high-quality material, document types were restricted to research publications.

Sixty-five (65) papers were reviewed under the elevated temperature category after thirty-three (33) documents were screened during manual filtering for their propensity to fall under the post-fire category and other irrelevant materials, duplication in the search list, and inaccessibility to online copy. Additional four (4) were manually collected from other sources and recommendations; therefore, a total of sixty-nine (69) papers involving CFS exposed at elevated temperatures were reviewed.

Following the final screening, Fig. 1 provides a summary of the annual publications. According to the graph, 2022 has the highest publications on CFS higher temperature, with 20 papers. The year 2017 had the fewest publications, with just one study conducted for that year.

2.2. Text mining using VOS viewer

After the last screening, the search results were exported as comma-separated values files or.csv files. After that, the co-occurring terms depicted in Fig. 2 were mapped using the exported.csv file in the VOS Viewer program. Co-occurring word clustering from the VOS viewer was utilized to help develop combination themes for CFS post-fire and under high temperatures.

Three clusters were created based on the VOS viewer mapping results from Fig. 2. Three subtopics were extracted from the three clusters: a. Finite element analysis in a fire condition, b. Exposure experimental results, and c. Member connections. Specific terminologies like stainless steel, sheathing, walls, and LSF walls were not taken into consideration while other material types were being considered.

3. CFS characteristics and performance at elevated temperature

3.1. Finite element analysis (FEA) in fire condition

Several authors have concentrated on research on CFS characteristics at increased temperatures through Finite Element Analysis, intending to examine its behavior or validate current design predictions by a code or previous research for applicability in a specific CFS scenario. Researchers used advanced tools like ABAQUS, ANSYS, and SAFIR to conduct a meticulous study. However, experimental data of CFS steel must be accessible and gathered either by the authors doing the experiments themselves or by referencing earlier experimental data provided by previous studies for FEA to be carried out. The FEA at elevated temperatures conducted by previous studies is further grouped into CFS compression members, CFS flexural members, and other CFS systems.

3.1.1. FEA for CFS compression members

Increased temperature FEA of members under compression conducted by different researchers is divided into two approaches: transient state and steady state. In the steady state, the sample is initially applied with heat to the needed temperature, then followed by the application of load to the member till failure. In contrast, a transient state condition, a more realistic scenario, is wherein the member is first subjected to the desired load, followed by the application of increasing temperature until failure [21]. Several researchers conducted a steady state approach in FEA where their studies aim to investigate the CFS column behavior at elevated temperatures and verify the adequacy of a prediction equation in calculating a specific CFS property. Their researches vary on (a.) CFS section profiles, (b.) steel grades, (c.) software and shell element used, (d.) column support conditions, (e.) range of temperature

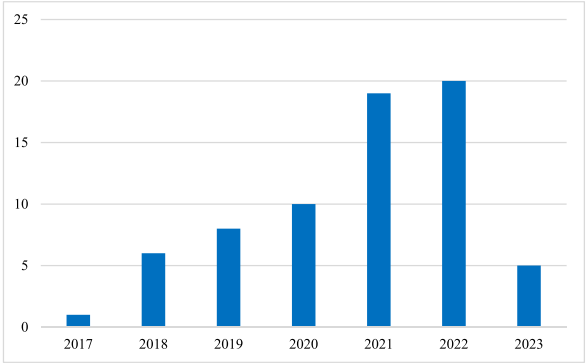

Fig. 1. Publications per year for CFS elevated temperature.

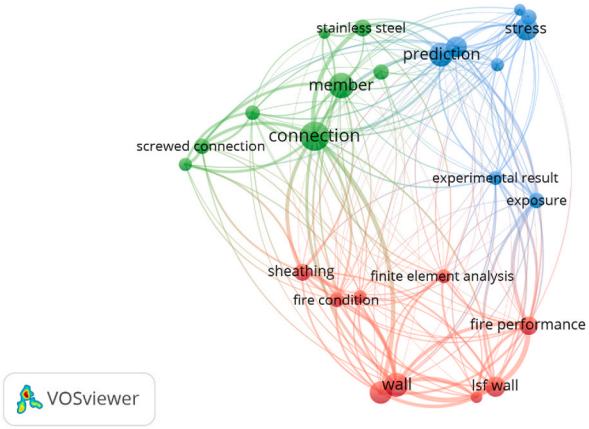

Fig. 2. Mapping for co-occurring keywords for cold-formed steel elevated temperature from VOS Viewer.

increase, (f.) investigated property, and (e.) the prediction equations from different codes or prior research being studied. Common codes that were verified are Australian Standards/New Zealand Standards (AS/NZS), British Standards (BS), Indian Standards (IS), American Society of Civil Engineers (ASCE), Eurocode (EN or EC), American Institute of Steel Construction (AISC) and American Iron and Steel Institute (AISI) or North American Standards (NAS). A summary showing important details of the elevated temperature FEA studies for CFS under compression conducted under steady-state conditions is shown in Table 2.

In terms of the transient state condition, Senthilkumar and Kumar performed an FEA using ABAQUS with an S4RT shell element with a mesh size of 17.5 mm to examine how the CFS compression members using S280 GD steel-lipped channels behaved in a transient state. According to their research, the peak and critical temperatures drop with a rise in the width-to-thickness ratio of roughly 7.0% and 7.5%, respectively. Columns with slenderness ratios higher than 150 tend to collapse at higher temperatures compared to columns with lesser than 150 slenderness ratios due to global buckling predomination in more slender columns [48]. Senthilkumar et al. using also the same FEA software and shell conditions concentrated on the application of non-uniform transient state conditions with changing load conditions on CFS compression members. Using S280 lipped channels as columns subjected to three non-uniform distributions of temperature wherein the lowermost temperature is 25%, 50%, and 75% of the uppermost temperature, they discovered that in comparison to columns with uniform thermal distribution, the columns' peak and critical temperatures with 50% non-uniform thermal dispersion rise by roughly 28% and 24%, respectively, and that the uniform thermal dispersion design is conservative with a rise in initially applied load, maximum limiting force intensification, and the peak and critical temperature reduction due to material deterioration [21].

3.1.2. FEA for CFS flexural members

Several research works have been on the FEA of CFS flexural members or beams in conditions that are in a steady state or transient state. For the prior investigations involving steady-state conditions, a summary in Table 3 is presented, wherein the key information such as (a.) CFS section profile, (b.) steel grades, (c.) loading conditions, (d.) range of temperature increase, (e.) software and shell element details used, (f.) examined properties, and (g.) prediction equations established by various references and earlier studies were presented.

Finite element analysis studies that concentrated on the transient state condition for CFS beams include those by Alabi-Bello et al., where their simulated FEA, utilizing ABAQUS with S4R shell and 5 mm mesh size, resulted in the creation of a Direct Strength Method (DSM) procedure in designing CFS beams that are transversely loaded and have local and distortional buckling failure vulnerability at high temperatures. Their study's main conclusions are that for thin-gauged steels with irregular cross-sectional distributions of elevated temperatures, DSM is an appropriate technique and that the current AISI S100-16 [27] DSM specifications are accurate enough to calculate local buckling capacity but overestimate the value for distortional buckling, leading to the suggestion of modified DSM equations [69]. On the other hand, DSM's validity was also checked by a prior study of Ananthi et al. when they utilized it in predicting the ambient.

temperature axial compression of CFS built-up section consisting of unequal angles with intermediate stiffeners and found that it is conservative by 5% and 7% on the average when used in its axial capacity prediction [70]. Lastly, Naser and Degtyareva. focused on the C-shaped CFS beams with slotted webs' response to temperature-induced shear-based instability. The obtained results showed that, at high temperatures, the channel depth and web perforation pattern considerably impact the CFS channels with slotted webs' shear response [71]. (Legend: C – Lipped Channel, U – Unlipped Channel)

3.1.3. FEA for light steel framing (LSF)

The increased temperature behavior of LSF has been the concentration of many types of research, where the CFS is examined as a part of a wall, ceiling, or floor frame coupled to a sheathing using FEA. From these earlier studies, different research circumstances were investigated for the evaluation of LSF properties at high temperatures.

Table 2
Summary of prior FEA for CFS compression members at steady-state condition.

Research	Year	CFS Section	Steel Grade	Tempera-ture Range	FEM Software/Shell Element/Mesh Size	Support Condition	Property Investigated	Design Predictions Checked
Kumar et al. [22]	2023	Rectangular Hollow Section (RHS)	YSt-355FR (0.1% Mo)	20°C–800 °C	ABAQUS/C3D8R/10 × 10mm	Fixed Ends	Axial Capacity	EC3 [23]
Liu et al. [24]	2022	Square Hollow Section (SHS), RHS	Austenitic stainless steel SUS316	20°C–900 °C	ABAQUS/S4R/20 × 20mm	Released rotation at minor axis for both ends, but axial displacement released in one end	Bearing Capacity	EN1993-1-2 [23]
Fang and Chan [25]	2022	SHS, RHS	S355, S450, S700, S900	20°C–800 °C	ABAQUS/S4R/Same with sample plate thickness (4–10 mm)	Fixed Ends, Pinned Ends	Axial Capacity	EN1993-1-2 [23], AISC 360 [1]
Yan and Gernay [26]	2022	RHS, SHS	Dual Phase-700, Martensitic-1200, G450	20°C–700 °C	SAFIR/not stated/3 × 3mm, 10 × 10mm	Fixed Ends	Local buckling capacity	AISI S100–16 DSM [27]
Fang et al. [28]	2022	Back-to-back Channel Sections	G250	20°C–700 °C	ABAQUS/S4R/5 × 5mm and 10 × 10mm	Pinned Ends	Axial Capacity	AS/NZS 4600 – EWM and DSM [29], AISI S100-16 [27]
Rahnavard et al. [30]	2022	Concrete filled built-up Section: 2C + 2U and 2C+2U Partially Embedded	S280GD + Z	20°C–700 °C	ABAQUS/DC2D4/not stated	Not Stated	Concrete and Steel Temperatures	EN1994-1-2 [31]
Bicelli et al. [32]	2021	Channel, Lipped Channel, Hat, Rack, Sigma	G250, G450, G550	20°C–800 °C	ANSYS/SHELL181/5 × 5mm	Fixed Ends	Flexural-torsional behavior	Dinis et al.'s Modified DSM [33]
Huang et al. [34]	2021	SHS, RHS	Austenitic (EN1.4301), duplex (EN1.4462), and lean duplex (EN1.4162)	24°C–960 °C	ABAQUS/S4R/10 × 10mm	Not Stated	Beam-Column Capacity	ASCE 8-02 [35], AS/NZS 4673 [36], EC3 Part 1.2 [23], EC3 Part 1.4 [37], Arrayago et al.'s DSM [38]
Arrais et al. [39]	2021	Lipped Channel, Sigma	280, 320, 355 and 460 MPa	350 °C, 500 °C, 600 °C	SAFIR/not stated/not stated	Pinned Ends	Ultimate load-bearing capacity	EC3: Part 1–2 - Annex E [40], EC3: Part 1–2 - French National Annex [44]
Rokilan and Mahendran [45]	2021	Lipped Channel	G150, G250, G450, G550	20°C–700 °C	ABAQUS/S4/3 × 3mm	Fixed Ends	Proportional limit stress - yield strength nonlinearity relation, stress, local buckling capacity	AS/NZS 4600 - EWM and DSM [32]
Rokilan and Mahendran [46]	2021	Lipped Channel, SHS	G150, G250, G450, G550	20°C–700 °C	ABAQUS/S4/5 × 5mm, 5 × 10mm	Fixed and Pinned Ends	Global buckling behavior, axial capacity	AS/NZS 4600 [32],AS/NZS 4100 [47],EN1993-1-2 [27]
Yang et al. [41]	2020	Built-up box sections (2C and 2U)	Q345	20°C–800 °C	ABAQUS/S4R, DS4 and DC2D4/10mmx10mm	Fixed Ends	Axial restraint, load ratio, rotational restraint influence on fire resistance	NONE
Mohammed and Afshan [42]	2019	SHS, RHS, Circular Hollow Section (CHS)	Ferritic (EN 1.4003), Duplex, and Austenitic (EN 1.4301) Stainless	20°C–800 °C	ABAQUS/S4R and DS4/ minimum of 10 elements across plates	Fixed and Pinned Ends	Flexural buckling capacity	EN1993-1-2 [27],SCI Stainless Steel Design Manual [43]
Huang and Young [44]	2019	SHS, RHS	Lean Duplex Stainless Steel (EN 1.4162)	24°C–900 °C	ABAQUS/S4R/not stated	Pinned Ends	Axial Capacity	AS/NZS 4673 [39],ASCE 8-02 [38],AISI S100 -DSM [23], EC3: Part 1–4 [45]
Landesman et al. [46]	2019	Lipped Channel, Rack section	550 MPa	20°C–600 °C	ANSYS/SHELL 181/not stated	Fixed Ends	Distortional ultimate Stress	Current DSM Methods [47]

Table 3
Summary of prior FEA for CFS flexural members at steady-state condition.

Research	Year	CFS Section	Steel Grade	Tempera-ture Range	FEM Software/Shell Element/Mesh Size	Loading Condition	Property Investigated	Design Predictions Checked
Fang et al. [49]	2023	Channels with Web Holes	S690QL	20°C–800 °C	ABAQUS/S4R/5 mm	End-One Flange	Web Crippling	AISI S100-16 [27], AS/NZS 4673 [36]
Li et al. [50]	2022	SHS, RHS	S700, S900	20°C–1000 °C	ABAQUS/S4R/not mentioned	Not stated	Web Crippling	AISI S100-16 [27], EN 1993-1-3 [51], Zhou and Young [52], Li and Young's DSM [53]
Fang et al. [54]	2021	Channels with Web Holes	G250, G450	20°C–700 °C	ABAQUS/S4R/ 5mmx5mm	Interior One Flange (IOF)	Web Crippling	Lian et al. Reduction Factor Equation [55,56]
Arrais et al. [57]	2021	Sigma Cross Section	280, 320, 355, 460 MPa	350 °C, 500 °C, 600 °C	SAFIR/not stated/5 × 5mm, 10 × 10mm, 25 × 25mm	Non-Uniform and Uniform flexure	Bending Resistance, Lateral-Torsional Buckling behavior	EC3: Part 1–2 - Annex E [23], EC3: Part 1–2 - French National Annex [58]
Cai et al. [59]	2021	SHS, RHS	Lean Stainless Duplex Steel (450 MPa)	22°C–950 °C	ABAQUS/S4R/2 × 2mm and 10 × 10mm	Interior-One-Flange (IOF), Interior-Two-Flange (ITF), Interior loading (IL)	Web Crippling	AISI S100-16 [27], EC3-1.3 [51], ASCE 8-02 [35],AS/NZS 4673 [36]
Cai et al. [60]	2021	SHS, RHS	Lean Stainless Duplex Steel (450 MPa)	22°C–950 °C	ABAQUS/S4R/2 × 2mm and 10 × 10mm	End-One Flange, End-Two Flange, and End Loading	Web Crippling	AISI S100-16 [27], EC3-1.3 [51], ASCE 8-02 [35],AS/NZS 4673 [36]
Kumar et al. [61]	2021	Channels with Web holes	G250	20°C–700 °C	ANSYS/SHELL 181/3 × 3mm, 5 × 5mm	End-Two Flange	Stress-strain relationships	Uzzaman et al. web crippling capacity equation [62]
Li and Young [63]	2019	SHS, RHS	700 MPa and 900 MPa	20°C–1000 °C	ABAQUS/S4R/5 × 5mm, 12 × 12mm	Not Stated	Stress-strain relationships, Slenderness Limits	EN 1993-1-1 [64],Ma et al.'s Slenderness Limits Proposal [65], ANSI/AISC 360 [1], AISI S100-16 [27]
Huang and Young [66]	2018	SHS, RHS	Lean Stainless Duplex Steel (450 MPa)	24°C–900 °C	ABAQUS/not stated/not stated	Not Stated	Flexural capacity	ASCE 8-02 [35], AISI 4763 [36], EC3 1–4 [67], Gardner & Theofanus EC3 [68], AISI S100-16 – DSM [27]

In the investigation of LSF wall frame performance under extreme temperatures, Peiris and Mahendran developed an improved single-stud FEA model of LSF walls subjected to combined compression and bending while being exposed to fire to ease the demanding computations in modeling. Material and geometrical non-linearities, contact interactions, and explicit modeling of gypsum plasterboard sheathing were integrated into their model, and it was found to be capable of predicting FRLs of LSF walls under combined axial and lateral loads [72]. In the study by Samiee et al., the wall modules' time-temperature profiles generated from their thermal investigation were used to run a structural FEA model under transient state conditions. The findings demonstrated that sheathing is a critical factor in the wall's fire resistance and substantially influences their fire resistance rating (FRR), and so is raising the stud depth. Additionally, expanding the LSF wall's stud flange width increases the wall's FRR against fire without changing the wall's thermal behavior or temperature distribution [73]. Through the adoption of a tension spring as a boundary condition simulation, Chen and Ye's research proposed a simplified calculation model using FEA to present the fire performance of CFS composite walls accurately and efficiently. This model limits the axial thermal expansion of the studs at high temperatures. The results presented that the formulated simplified calculation model is capable of simulating fire performance and accurately predicting the lateral deflection of the externally sandwiched cold-formed steel composite walls. In addition, it was shown that the vertical load ratio and temperature rise rate are the two most important elements determining the lateral deformation of walls [74]. Ariyanayagam and Mahendran performed LSF load-bearing walls standard fire tests with gypsum board sheathing that were employed in low-rise building construction to examine the influence of utilizing low-strength steel studs having 339 MPa ambient temperature yield strength, noggings, and cavity insulation through FEA modeling. The study's findings demonstrated that low-strength steel stud walls' fire resistance level (FRL), when compared to high-strength steel stud walls, is roughly 25% lesser in the common load ratio range while there is a decrease in their critical hot flange temperatures [75]. The study showed that Eurocode 3 Part 1.2 CFS reduction factors [33] offered similar FRLs for steel stud walls, whether high or low-strength [75].

Several research works utilizing FEA have focused on investigating LSF behavior installed with various sheathings and insulations under fire exposures. Perera et al. created an FEA model for LSF walls to replicate full-scale tests in examining the performance in fire of LSF conventional and modular schemes with various cavity insulations. From their study, it was found that the 0.4 cavity insulation ratio is the most effective when concerning the structural FRL while yielding acceptable energy performance at a lower cost of materials, and various innovative conventional and modular LSF walls have been developed, having less energy use up to 70% [76]. Abeysiriwardena and Mahendran investigated the influence of out-of-plane restraints given by plasterboard sheathing using a single stud FEA model with simplified boundary conditions and concluded that the FRL of the walls is considerably enhanced by the out-of-plane restraints provided by gypsum plasterboard with 16 mm thickness. Their research has also established suitable out-of-plane restraint values recommended for use in the numerical analysis of walls with single and double plasterboard sheathings [77]. Tao et al. presented an FEA modeling of LSF walls using ANSYS to study the benefit of utilizing RHS/SHS studs walls that are cavity insulated and to investigate whether steel quality and stud depth could alter the LSF walls' fire resistance capacity. Results manifested that localized fall-off of plasterboard is crucial to the behavior of walls in fires because it greatly speeds up temperature increase in the steel studs nearby and creates hot spots in the studs. Moreover, it was discovered that the hollow chamber of RHS/SHS speeds up the process of heat transmission between the cold and hot flanges of the stud, preventing discrepancies between them and reducing thermal bending deformations [78]. Steau and Mahendran used ABAQUS for the thermal behavior examination of LSF floor-ceiling schemes with various arrangements, which featured gypsum plasterboard, rockwool fiber insulation, steel sheathing, structural plywood, and lipped channel and rectangular hollow flange channel section joists attached with rivets. According to the study, the innovative LSF floor-ceiling scheme supplemented with sheathing of thin steels outperformed the conventional systems. Moreover, because the cavity side steel sheathing remained for extended periods at lower temperatures than those for the fireside steel sheathing, the rate of thermal radiation heat transmission in the cavity was eased; as such, further improvements were seen in thin steel sheathing usage on plasterboard's both sides. Lastly, it was found that cavity insulation use demonstrated detrimental effects [79].

In validating existing design rules' applicability to LSF walls through FEA, the research by Rokilan and Mahendran examined the accuracy of the effective width method (EWM) and direct strength method (DSM) in the present AS/NZS 4600 [29] design equations due to difficulties in their applications to CFS lipped channel studs in wall schemes that are subjected to elevated temperature distributed non-uniformly. The research then streamlines the calculations while maintaining the load ratios' accuracy (ratio of elevated to ambient temperature capacity). While their research found both EWM and DSM are accurate, DSM was less accurate than EWM. As a result, they suggested a streamlined DSM design procedure based on uniform temperature and incorporating mechanical properties of the hot flange, and a hot and cold flange temperatures correction factor, yield strength, stud length, and stud depth [80]. In another study, Ariyanayagam and Mahendran's work showed that Eurocode 3 Part 1.2 CFS reduction factors [33] offered similar FRLs for steel stud walls, whether high or low-strength [75].

Studies involving LSF used as a floor system have been undertaken. Perera et al. did a numerical modeling of conventional and modular LSF floor panels through ABAQUS to investigate their fire performance. Their model incorporated 12.5 mm thick gypsum board ceiling boards and cavity insulations. It was found that the addition of the ceiling board increased the structural and insulation FRL of the floor panels by a considerable time of 30 min, and that the FRL performance also goes with the insulation volume provided. In addition, their study concluded that ceiling insulations in modular panels are recommendable and more efficient than cavity insulations in the conventional panels [81]. Gateeshgar et al. developed a 2D and 3D FEA model of conventional and modular LSF panels that utilize optimized CFS sections as floor joists. With the use of ABAQUS, their study found that the modular panels show considerable structural and insulation FRR of more than 4 h than the conventional panels which could be attributed to the modular panels' separate floor and ceiling panel nature. Their study also reflected that the fire performance of the floor panels could be improved with the use of the optimized CFS profiles [82].

Table 4
Summary of previous experimental tensile tests for CFS at elevated temperature.

Research	Year	Steel Grade	CFS Section	Testing Condition	Temperature Range	Property Investigated	Design Predictions Checked
Kumar et al. [22]	2023	YSt-355-FR (0.1% Mo)	RHS	Steady State	20 °C–800 °C	E, proportional limit strength, f_y, f_u, fracture strength, ε_y, ε_u, ε_{frac}	EC-3 [23], AS 4100 [87], AISC 360 [1], BS 5950 [88], IS 800 [89]
Kumar et al. [90]	2022	YSt-355-FR (0.126% Mo)	RHS	Steady State	20 °C–800 °C	Proportional limit strength, f_y, f_u	EC-3 [23], AS 4100 [87], AISC 360 [1], BS 5950 [88], IS 800 [89]
Liang et al. [91]	2022	Q345	Flat and Corner parts of a Channel	Not mentioned	20 °C–800 °C	E, f_y	EC-3 [23], AS 4100 [87], AISC 360-10 [1]
Pieper and Mahendran [92]	2021	G550	Corrugated cladding, trapezoidal cladding	Steady State	20 °C–600 °C	f_y, f_u, 0.05% proof stress, ε_u, ε_{frac}	AS/NZS 4600 [29]
Yan et al. [93]	2020	Mild steel (MS-395), High strength low-alloy steel (HSLA- 700), and AHSS (DP340, DP700, MS-1030, and MS-1200)	Steel sheets	Steady State and Transient State	20 °C–700 °C	E, f_y, yield stress at strain levels of 0.5%, 1.0%, 2.0%, f_u, ε_{frac}	EC-3 [23], AISC 360 [1]
Chen et al. [94]	2020	G550	CFS studs	Steady State	20 °C–900 °C	E, f_y, f_u	NONE
Rokilan and Mahendran [95]	2020	G300, G550	Lipped channels, floor decks	Steady State	20 °C–700 °C	f_y, f_u, proportional limit, stress at 2%, 0.05%proof stress, ε_u, ε_{frac}	AS/NZS 4600 [29]
Singh and Singh [96]	2019	YSt-310	SHS, RHS	Steady State	20 °C–800 °C	f_y, stresses at 0.5%, 1.0%, and 2.0%, f_u, ε_u, ε_{frac}	EC-3 [23], AS 4100 [87], AISC 360 [1], BS 5950 [88], IS 800 [89]
Imran, M. et al. [20]	2018	G350	SHS, RHS, CHS	Steady State	20–800 °C	f_y, stress at 2% strain, E, f_u, ε_u	BS 5950 [88], EC3 [23], AS 4100 [87], AISC 360-10 [1]
Li and Young [97]	2017	700 MPa, 900 MPa	SHS, RHS	Steady State and Transient State	21 °C–1000 °C	Thermal elongation, E, f_y, f_u, ε_u, and ε_{frac}	EC3 [23], AISC 360 [27], AS 4100 [87], BS 5950 [88], Chen and Young's equation [98]

Legend: E = Elastic modulus, f_y = yield stress/0.2% proof stress, ε_y = yield strain, f_u = ultimate strength, ε_u = ultimate strain, ε_{frac} = fracture strain.

3.1.4. FEA for CFS structure

For FEA conducted involving a CFS structure, Yan and Gernay demonstrated a method for CFS structures fire design and applied it to the assembly of columns obtained from a single-story metal warehouse model structure designed conforming to U.S. building codes. The establishment of performance goals, design fires, FEA heat transport assessments, and structural analyses using both the DSM and FEA via SAFIR are all included in the fire design procedure. The findings demonstrate that the analysis method of design provides the requisite performance while promoting the flexibility and effectiveness of the design. Moreover, the DSM's applicability with the proper retention factors to assess the higher temperature response was confirmed by the FEA. Because of the low magnitude load brought on by the load combinations in the fire event, excluding the wind, the CFS columns maintain more stability than their prescribed rating. Therefore, analysis techniques can be utilized to show better performance than the applicable fire resistance rating for structures that are minimally loaded in a fire condition [83].

3.1.5. FEA for CFS high-strength steels

Xia et al. performed a thorough numerical investigation on the stress-strain correlations of two dual-phase advanced high-strength steel AHSS (340 and 700 MPa) and two martensitic AHSS (1030 MPa and 1200 MPa) at high temperatures from 20 °C to 700 °C limits, and after cooling down. The composition of the AHSS, the strength of the steel, the testing procedure, and the highest temperature were discovered to impact the stress-strain behaviors. In addition, two stress-strain modes were identified in their research: a gradual strain hardening development with no definite yield point, known as Mode 1, that occurs at or below 200 °C, and a sharp strain hardening development with a definite yield point, known as Mode 2, that happens at 300 °C or higher test temperatures [84].

3.2. Elevated temperature exposure experimental results

To examine the characteristics of various CFS sections under extreme temperature conditions or to verify the validity of an existing design prediction equation, researchers have conducted experiments on these sections. Although experimental methods are more expensive than FEA methods, unlike FEA methods where the input data must be based on existing experimental data or prior research to be completed, experimental techniques do not require previous studies for input. Prior experimental investigations for CFS are presented based on the tests conducted and the systems involved.

3.2.1. Experimental tensile tests for CFS at exposure to elevated temperature

The primary goal of experimental tests on various CFS sections and grades is to understand their behavior by determining their mechanical properties using the tensile test at elevated temperatures and confirming the applicability of a design prediction in the CFS specimen properties under investigation. Further, in tensile tests, the stress-strain response of the CFS section is investigated which is necessary before its adaptation as a structural member since the cold-forming process it undergoes induces modifications among the sections' regions [85]. When subjected to high-temperature scenarios with distinct elevated temperature ranges adopted by the researchers, these experimental tests might also be either steady state or transient state. The summary of the experimental tensile testing for CFS at elevated temperatures done by earlier writers is presented in Table 4. In the table, significant information such as (a.) steel grade, (b.) CFS section, (c.) testing condition, (d.) temperature range, (e.) property investigated and (f.) design predictions checked are shown. For experimental investigations of lean duplex, austenitic and ferritic steels with hollow CFS profiles, and steel grades that are not found in Table 4, an earlier exploration at ambient temperature scenario was conducted by Afshan et al. to validate the Australian code and Eurocodes [86].

3.2.2. Experimental compression test for CFS at exposure to elevated temperature

Yang et al. performed experimentation in full-scale on the fire responses of built-up box columns loaded axially using Q345 CFS for the compression test of CFS at elevated temperature with various scenarios associated with the influences of load ratio, heating rate, and temperature allocation pattern. According to the test results, raising the load ratio caused a considerable drop in the member critical temperatures, significantly decreasing the columns' ability to withstand fire [99].

3.2.3. Other experimental tests for CFS at elevated temperatures

Other experimental tests which involve the elevated temperature behavior of CFS systems not mentioned in the previous sections have been implemented in prior research works. In investigating the CFS claddings' pull-through capacity subjected to a combination of fire and wind action, Pieper and Mahendran created a small-scale test setup simulating wind suction pressure on the wall claddings and crest-fixed CFS roof and, at the same time, being subjected to increased temperatures. For buildings located in bushfire-prone areas, this is essential to consider for the safe design of these buildings. Three frequently used cladding profiles formed using high strength (G550) CFS with 0.42 mm thicknesses were subjected to experiments at ambient temperature and higher temperatures, and crucial localized crests' pull-through failure under the screw heads was examined. The results show that the pull-through capacity decreased at varying rates depending on the cladding profile and the temperature [100]. Concerning creep behavior, Liu et al.'s experimental investigation of using 1.0 mm thick G550 CFS and a creep duration of 4 h revealed that the G550 CFS creep curves were noticeably distinct from those of hot-rolled high-strength Q550 and Q690 steels at high temperatures. Additionally, creep rupture would occur in the coupon samples of G550 CFS that displayed tertiary creep during the testing. Finally, the results of the transient-state differed from steady-state testing for the G550 CFS strain, with the creep strain significantly contributing to this variation [101]. When it comes to thermal property investigations, Steau et al. presented a series of experimental investigations to confirm the accuracy of the thermal characteristics in Eurocode 3 Part 1.2 for the LSF components. Thermal property tests on three

different carbon steel types, specifically Grade 140 steel, Grade 300 steel, and Grade 500 steel, were done to ascertain their relative density, constant pressure specific heat, thermal diffusivity, and thermal conductivity. As a result of their chemical makeup and carbon content impact, test findings revealed inconsistencies in thermal conductivity and specific heat of all three types of carbon steels between the measured thermal property data and the carbon steels' Eurocode 3 Part 1.2 model [102].

In a full-scale experimental test of a building, Roy et al. investigated the collapse behavior of a CFS-based single-story structure with dimensions of 8 m by 10 m having a height to roof eaves of 2.15 m when exposed to fire using an ISO curve. The experimental investigation was accompanied by FEA modeling using ABAQUS with DS4 shell element for validation. The results indicated that collapse was achieved at temperatures of 622.5 °C for the experimental study and at 628.2 °C for the FEM part. The collapse of the roof was perceived after 8 min of substantial fire intensification has begun. The CFS wall/truss system collapsed after 21 min and 30 s. It was observed that the walls of the building protected by gypsum did not fail at the end of the test. The 15 mm thick gypsum board protected the CFS stud in one of the building walls from a 45% increase in temperature and a time delay of 46% [103].

3.3. Member connections at elevated temperature

The behavior of member connections of CFS has been explored in previous research works. Common connection used in the CFS have screwed connections and their behavior at high temperatures has been the subject of prior investigations. Vy and Mahendran explored the screwed connections' shear behavior and capacity, in which they examined these connections being employed in built-up CFS members at increased temperatures of 700 °C. It featured a series of tilting and bearing shear investigations on screwed connections utilized to connect two single channels resulting in a CFS member that is built-up back-to-back. Their research has verified the validity of the AS/NZS 4600 [29] design formulae for the ambient temperature screwed connections' bearing and tilting resistance used in built-up CFS members. The study also found that, when combined with their suggested formulae for the reduction factor, similar design equations may be employed to forecast the screwed connections' bearing and tilting strengths when exposed to high temperatures [104]. Chen et al. presented single-shear experimentation of screwed connections of CFS-to-steel at ambient and increased temperatures subjected to both transient state and steady-state conditions. It has been verified that the AISI S240-15 [105] minimum loaded edge distance of three times the screw's nominal diameter is sufficient for the design against the shear of screwed connections of CFS-to-steel at high temperatures. Four failure modes—tilting plus bearing, tilting plus edge tearing, tilting plus shearing, and pure shearing—were identified in their investigation. The shear strength of tilting plus edge tearing and tilting plus bearing failure turned out to be lower than that of tilting plus shearing and pure shearing failure [106]. Yang et al. conducted an experimental and analytical investigation on box-shape CFS built-up columns consisting of four Q355 CFS channels screwed together and exposed to high temperatures. The results indicated that screw spacing considerably influenced the fire performance of the CFS section since specimens with smaller screw spacing showed higher critical temperature. They found that the composite action of the built-up section was more effective for specimens with 150 mm screw spacing. Moreover, end fastening groups in the built-up section have demonstrated a 1.4%–3.2% improvement in the section's performance which is deemed to be inefficient for engineering purposes [107]. In contrast, based on a prior investigation by Ananthi et al. at ambient temperature axial capacity of a built-up section of 4-channel columns, it was observed that for short stub columns, the doubling of screw fastener spacing would lead to a reduction of axial capacity by 2%–18% [108].

In terms of a study of bolted connections in CFS, in the experiment by Cai and Young, connections with single shear bolts used in thin sheet steel (TSS) at high temperatures were examined. The connection specimens with end distance variation were made using TSS 1.90 mm G450 and 0.42 mm G550. The maximum loads were discovered to rise with the end distance increment of up to three times the bolt diameter. The experimental results also demonstrated the conservative nature of the predictions for CFS structures made by the AS/NZS 4600 [29], EC3-1.3 [51], and NAS [27], with the AS/NZS making the most accurate and precise projections possible [109]. Using a finite element model, Cai and Young reported an elevated temperature computational analysis of connections made of cold-formed stainless steel (CFSS) and single shear bolts. The computed nominal bearing capacities using the specifications of stainless steel from AS/NZS 4673 [36], ASCE 8-02 [35], and Eurocode 3 Part 1–4 [37] were compared to the FEA calculated connection bearing strengths. It was discovered that using the equations from the current codes would result in a conservative value of bearing strengths. Consequently, a proposed modified design rule was suggested by this study for more accurate calculations [110].

For the investigation of the behavior of connections of LSF boards, Batista Abreau et al. used steady-state experimentation to examine the in-plane shear and pull-through capability of CFS members connected to oriented strand board (OSB) and gypsum board at temperatures up to 400 °C. It was determined that both gypsum and oriented strand board sheathing's mechanical stiffness and strength of CF steel-to-sheathing connections considerably decrease with temperature. Only 33% of their ambient temperature stiffness and strength in shear, and 25% of their ambient temperature capacity in pull-through, are exhibited by connections to gypsum board at 250 °C. On the other hand, OSB has kept 40% of its shear and pull-through strength at 200 °C, and at 350 °C and higher, it offers no mechanical support [111].

4. Key findings

This paper reviewed present research works on the performance of CFS at elevated events. A total of sixty-nine (69) articles published in the literature from 2017 to 2023 were reviewed. A general trend is that the research projects focusing on these topics have increased over the years. Moreover, prior research regarding the elevated temperatures performance of CFS has primarily focused also on its properties as a beam or column rather than the behavior of connections used in CFS. The following key findings based on the review of prior studies are summarized.

4.1. Finite element analysis

Primary investigations using finite element analysis of CFS utilized as compression, flexural, and framing systems commonly concentrated on the validation and applicability of current design codes particularly AISI S100, Eurocode, and AS/NZS 4600. When it comes to compression members exposed to high temperatures, the Eurocode provisions are generally conservative in predicting the capacities except for austenitic stainless steels SUS316, slender lipped channels and sigma sections, ferritic, duplex, and austenitic (EN 1.401) steels. AS/NZS 4600 are found to be unsafe to be used in predicting lipped channels and SHS properties such as axial capacity, local and global buckling capacities, and proportional limit stress - yield strength nonlinearity relation, which resulted in suggested modification of the current design rules by Rokilan and Mahendran [112,113]. On the other hand, previous studies that tackled AISI S100 has found its code provisions to be conservative in dealing with local buckling capacities of SHS and RHS martensitic and dual phase steels and back-to-back channel sections. For flexural members, Eurocode also yielded conservative predictions for web crippling capacities, stress-strain relations, and flexural capacities of the lean stainless duplex steels. On the other hand, AISI S100-16 demonstrated unconservative results for web crippling capacity predictions on lean stainless duplex steels. Furthermore, AISI S100 and Eurocode have yielded inaccurate prediction results for the web crippling involving high-strength steels S700 and S900. With regards to the validity of the current design codes to the capacities of LSF walls at high-temperature exposure, AS/NZS 4600 could provide accurate prediction results of load ratios using EWM and DSM. Likewise, Eurocode is found to be accurate in predicting the reduction factors of LSF at elevated temperatures.

Finite element analysis was also employed in the investigation of the beneficial effects of using sheathings and insulation on LSF systems such as walls and floor panels through numerical simulations. Based on the previous studies, applying sheathings and insulations increases the fire capacities of the LSF systems. LSF wall systems investigated with FEA found that the fall-off of plasterboard is significant to the wall's fire performance. From an FEA developed in the simulation of conventional and modular LSF wall systems with cavity insulations, cavity insulations at 0.40 insulation ratio is the optimized set-up when dealing with the FRLs. In terms of floor panel systems, the usage of ceiling boards can improve the FRL of the floor panels by 30 min and the fire performance of the floor panels is proportionate to the insulation volume installed.

4.2. Experimental investigations

Like finite element analysis, in previous studies that conducted experimental investigations regarding CFS exposed to high temperatures, validation of the codified provisions has been their concentration and objective. AISC 360, EC3, BS5950, and AS 4100 do not correctly predict the yield strength factors of YSt- 355 0.126% and 0.10% Mo steels. In calculating cladding profiles of both corrugated and trapezoidal, the usage of AS/NZS 4600 is suitable for predicting their mechanical properties. In addition, AS/NZS 4600 can be used in predicting the reduction of the mechanical properties of cold rolled steel sheets, open CFS profiles, and floor decks. However, when applied to sections with high cold working levels, the code provisions could be too conservative. Lastly, EC3, AISC, and BS 5950 predictive rules based on hot-rolled sections are not applicable for use in CFS high-strength steels with yield strengths of 700 MPa and 900 MPa.

Several experimental investigations covering CFS insulations have arrived at various key conclusions primarily on the insulation they have included in the study. Brick veneer cladding improved LSF performance by resisting fire exposures [114]. SAP when used as CFS insulation aided in the improvement of LSF structural performance which could be credited to its capacity to absorb heat [115]. Other plasterboards such as gypsum plasterboards, perlite boards, and calcium silicate boards also improve the FRR of the LSF system due to their low thermal conductivity, high specific heat, and low bulk density [116]. Gypsum boards when used in LSF and exposed to high temperatures start to fall off at temperatures between 690 and 700° Celsius [117]. Experimental investigation on a full-scale one-story building exposed to fire has found that walls shielded by gypsum did not fail at the end of the test. The gypsum board provided in the structure protected the CFS studs from a 45% temperature rise and 46% of time delay.

4.3. Screw connections

For member connections which are primarily about screw connections, AS/NZS 4600 can be accurately used in predicting the bearing and tilting strength of screw connections at high temperatures provided that reduction factor formulae suggested by the study will be utilized [104]. In validating current design rules, the AISI S100 provision for screw connection minimum loaded edge distance is adequate for the calculation of the shear design of the connection. The North American Standards, Eurocode, and AS/NZS were found to be conservative in the prediction of the TSS failure modes where bearing and tear-out failure at different levels of temperature are involved. In stainless steels, ASCE, AS/NZS, and the European codes are discovered to be conservative in predicting its connections' nominal bearing capacities. On the other hand, from the study of built-up columns when exposed to high temperatures, screw spacing is crucial in the capacity of the built-up section when exposed to fire. It was concluded that smaller screw spacing will induce a more effective composite action in built-up sections.

5. Current research limitations and future direction

While it is evident that the research involving CFS behavior at elevated temperatures has significantly developed, there are research gaps that need to be addressed based on the conducted literature review and suggested as future work.

- Based on the literature gathered, different types of steel used as CFS in structures vary regionally depending on the design restrictions set by the incumbent structural code or standard in that country. For example, G300 and G250 steels are utilized extensively in Europe, North America, and Australia [118]; S280 and S350 steels are suggested by the Chinese code [118]; JIS STKR400 are used in Japan [119]; and YSt-310 are commonly used in India [96]. Thus, it is recommended for future studies to conduct investigations on the elevated temperature properties of newly developed steel grades and validate the properties using the design rules by the region's governing code. This directive will be essential in developing or amending the policies of the region's fire design involving CFS.
- Future investigations are also recommended to concentrate on other CFS systems when exposed to elevated temperature events such as the presence of slots in the webs, built-up sections such as double box T-girders [120], and other irregular profiles such as angles, hats, sigma, and Z-sections since the bulk of the prior researches concentrated on channels and hollow sections.
- It is suggested that future studies investigate CFS performance under cyclic loading and fatigue at increased temperatures which was not extensively tackled in prior research works.
- Works involving riveted connections used in CFS exposed to fire have not also been explored, hence, could also be explored in the upcoming research works.
- In terms of full-scale investigation of structures which could be numerical or experimental, CFS-based structures' performance when exposed to fire and successive seismic loads simultaneously are yet to be explored. This would simulate a structure experiencing both a fire event and seismic aftershocks at the same time. This study could lead to the understanding of the behavior of structures when exposed to both fire and seismic events and could be significant for essential facilities.

Funding Information and Acknowledgment

This project is funded by the Department of Science and Technology (DOST) through the Science for Change Program (S4CP) – Collaborative Research and Development to Leverage Philippine Economy (CRADLE) and monitored by DOST -Philippine Council for Industry, Energy, and Emerging Technology Research and Development (PCIEERD) with Project No. 8739. The authors would like to acknowledge DOST, PCIEERD, the Department of Civil Engineering and Center for Engineering and Sustainable Development Research of De La Salle University, and Accutech Steel and Services, Inc. for their support on this paper.

Author contribution statement

All authors listed have significantly contributed to the development and the writing of this article.

Data availability statement

Data will be made available on request.

Declaration of competing interest

The authors declare the following financial interests/personal relationships which may be considered as potential competing interests.

References

[1] American Institute of Steel Construction (AISC), Specification for Structural Steel Buildings, American Institute of Steel Construction, Chicago, 2016.
[2] R. Kulkarni, V. Vaghe, Experimental study of bolted connections using light gauge channel sections, using stiffener/packing plates at the joints, Int. J. Eng. Res. Technol. 2 (2) (2013).
[3] G. Hancock, Cold formed steel structures: research Review 2013 - 2014, Adv. Struct. Eng. 19 (3) (2016) 393–408.
[4] D. Allen, History of Cold Formed Steel," Structure Magazine: Building Blocks, November Issue, 2006, pp. 28–32.
[5] S. Babu, S. Selvan, State of the art of the cold formed steel members, Mater. Today: Proc. 37 (2021) 3069–3073.
[6] W. Yu, R. LaBoube, H. Chen, Cold Formed Steel Design, John Wiley & Sons. Inc., New Jersey, 2019.
[7] Y. Halabi, J. Alhaddad, Manufacturing, applications, analysis and design of cold-formed steel in engineering structures: a review, International Journal of Advanced Engineering Research and Science 7 (2) (2020) 11–34.
[8] G. Hancock, Cold formed steel structures, J. Constr. Steel Res. 59 (4) (2003) 473–478.
[9] Y. Lee, C. Tan, S. Mohammad, M. Tahir, N. Shek, Review on Cold-Formed Steel Connections, The Scientific World Journal, 2014.
[10] G.B.G. Ananthi, State-of-the-art review on cold-formed steel channel sections under compression, J. Struct. Eng. 44 (1) (2017) 23–28.
[11] M. Javed, N. Hafizah, S. Memon, M. Jameel, M. Aslam, Recent research on cold-formed steel beams and columns subjected to elevated temperature: a review, Construct. Build. Mater. 144 (2017) 686–701.
[12] Y. Yu, L. Lan, F. Ding, L. Wang, Mechanical properties of hot-rolled and cold-formed steels after exposure to elevated temperature: a review, Construct. Build. Mater. 213 (2019) 360–376.
[13] A. Diaz, I. Cuesta, J. Alegre, d. Jesus, A.M. P, J. Manso, Residual stresses in cold-formed steel members: review of measurement methods and numerical modelling, Thin-Walled Struct. 159 (2021).
[14] H. Liang, K. Roy, Z. Fang, J. Lim, A critical review on the optimization of cold-formed steel members for better structural and thermal performances, Buildings 12 (34) (2022).
[15] M. Sani, F. Muftah, C. Tan, A state-of-the-art review on cold-formed steel roof truss system, Int. J. Civ. Eng. Technol. 9 (9) (2019) 746–758.
[16] P. Sharafi, M. Mortazavi, N. Usefi, K. Kildashi, H. Ronagh, B. Samali, Lateral force resisting systems in lightweight steel frames: recent research, Thin-Walled Struct. 130 (2018) 231–253.

[17] G. Di Lorenzo, A. De Martino, Earthquake response of cold-formed steel-based building systems: an overview of the current state of the art, Buildings 9 (11) (2019).
[18] F. Amsyar, C. Tan, C. Ma, A. Sulaiman, Review on composite joints for cold-formed steel structures, E3S Web of Conferences 65 (2018).
[19] N. Usefi, P. Sharafi, H. Ronagh, Numerical models for lateral behaviour analysis of cold-formed steel framed walls: state of the art, evaluation and challenges, Thin-Walled Struct. 138 (2019) 252–285.
[20] M. Imran, M. Mahendran, P. Keerthan, Mechanical properties of cold-formed steel tubular sections at elevated temperatures, J. Constr. Steel Res. 143 (2018) 131–147.
[21] R. Senthilkumar, C. Kumar, R. Saravanakumar, D. Kumar, Numerical study on restrained thermal elongation of cold-formed steel column subjected to non-uniform thermal loading under transient state, Fire Saf. J. 131 (2022).
[22] W. Kumar, U. Sharma, P. Pathak, Comparison of mechanical and structural performance of fire-resistant steels at elevated temperatures, Structures 48 (2023) 478–491.
[23] European Committee for Standardization (CEN), BS EN 1993-1-2:2005: design of steel structures – Part 1-2: general rules – structural fire design, in: *Eurocode 3*, Brussels, European Committee for Standardization (CEN), 2005.
[24] M. Liu, S. Duan, Y. Wu, S. Fan, Q. Xu, Fire resistance design of austenitic SUS316 stainless columns subjected to axial compression, J. Constr. Steel Res. 198 (2022).
[25] H. Fang, T. Chan, Behaviour and design of cold-formed normal- and high-strength steel SHS and RHS columns at elevated temperatures, Thin-Walled Struct. 180 (2022).
[26] X. Yan, T. Gernay, Local buckling of cold-formed high-strength steel hollow section columns at elevated temperatures, J. Constr. Steel Res. 196 (2022).
[27] American Iron and Steel Institute (AISI), North American Cold-Formed Steel Specification for the Design of Structural Steel Members (AISI S100-16), American Iron and Steel Institute, Washington, D.C., 2016.
[28] Z. Fang, K. Roy, D. Lakshmanan, P. Pranomrum, F. Li, H. Lau, J. Lim, Structural behaviour of back-to-back cold-formed steel channel sections with web openings under axial compression at elevated temperatures, J. Build. Eng. 54 (2022).
[29] Standards Australia, Australian Standard/New Zealand Standard (AS/NZS) 4600: Cold-Formed Steel Structures, Standards Australia, Sydney, Australia, 2018.
[30] R. Rahnavard, H. Craveiro, R. Simões, A. Santiago, Equivalent temperature prediction for concrete-filled cold-formed steel (CF-CFS) built-up column sections (part B), Case Stud. Therm. Eng. 35 (2022).
[31] European Committee for Standardization (CEN), Design of steel and composite structures, Part 1.2: structural fire design, in: ENV 1994-1-2, British Standards Institution: European Committee for Standardization, London, 2003.
[32] A. Bicelli, A. Landesmann, D. Camotim, P. Dinis, Flexural–torsional failure and DSM design of fixed-ended cold-formed steel columns at elevated temperatures, Thin-Walled Struct. 169 (2021).
[33] P. Dinis, D. Camotim, A. Landesmann, A. Martins, Improving the direct strength method prediction of column flexural–torsional failure loads, Thin-Walled Struct. 148 (18) (2020).
[34] Y. Huang, J. Chen, Y. He, B. Young, Design of cold-formed stainless steel RHS and SHS beam–columns at elevated temperatures, Thin-Walled Struct. 165 (2021).
[35] American Society of Civil Engineers (Asce), SEI/ASCE 8-02: Specification for the Design of Cold-Formed Stainless Steel Structural Members, American Society of Civil Engineers, Reston, Virginia, 2002.
[36] Standards Australia, Australian Standard/New Zealand Standard (AS/NZS) 4673: Cold-Formed Stainless Steel Structures, Standards Australia, Sydney, Australia, 2001.
[37] European Committee for Standardization (CEN), BS EN 1993-1-4:2006+A2:2020: design of steel structures – Part 1-4: general rules – supplementary rules for stainless steels, in: *Eurocode 3*, Brussels, European Committee for Standardization (CEN), 2020.
[38] I. Arrayago, K. Rasmussen, E. Real, Full slenderness range DSM approach for stainless steel hollow cross-section columns and beam–columns, J. Constr. Steel Res. 138 (2017) 246–263.
[39] F. Arrais, N. Lopes, P. Vila Real, Fire design of slender cold-formed lipped channel and sigma section members with uniform temperature under compression, Fire Saf. J. 122 (2021).
[40] European Committee for Standardization (CEN), Eurocode 3, in: EN 1993-1-2: Design of Steel Structures – Part 1–2: General Rules - Structural Fire Design, European Committee for Standardization (CEN), Belgium, 2005.
[41] J. Yang, Y. Shi, W. Wang, L. Xu, H. Al-azzani, Experimental and numerical studies on axially restrained cold-formed steel built-up box columns at elevated temperatures, J. Constr. Steel Res. 171 (2020).
[42] A. Mohammed, A. S, Numerical modelling and fire design of stainless steel hollow section columns, Thin-Walled Struct. 144 (2019).
[43] Steel Construction Institute, Stainless Steel Design Manual, fourth ed., 2017.
[44] Y. Huang, B. Young, Finite element analysis of cold-formed lean duplex stainless steel columns at elevated temperatures, Thin-Walled Struct. 143 (2019).
[45] European Committee for Standardization (CEN), BS EN 1993-1-4: 2006+A1: 2015: design of steel structures: general rules – supplementary rules for stainless steels, in: *Eurocode 3*, Brussels, European Committee for Standardization (CEN), 2015.
[46] A. Landesmann, D. Camotim, F. Silva, DSM design of cold-formed steel columns failing in distortional modes at elevated temperatures, International Journal of Steel Structures 19 (3) (2019) 1023–1041.
[47] B. Schafer, Review: the Direct Strength Method of cold-formed steel member design, J. Constr. Steel Res. 64 (7–8) (2008) 766–778.
[48] R. Senthilkumar, D. Kumar, Numerical studies on restrained cold-formed steel column subjected to transient thermal loading, Structures 32 (2021) 161–169.
[49] Z. Fang, K. Roy, D. Chandramohan, A. Yousefi, Y. Al-Radhi, J. Lim, End-one-flange web crippling behavior of cold-formed high-strength steel channels withWeb holes at elevated temperatures, Buildings 13 (266) (2023).
[50] H. Li, K. Zhan, B. Young, Web crippling design of cold-formed high strength steel SHS and RHS at elevated temperatures, Thin-Walled Struct. 180 (2022).
[51] European Committee for Standardization (CEN), EN 1993-1-3: design of steel structures - Part 1-3: general rules - supplementary rules for cold-formed members and sheeting, in: *Eurocode 3*, Brussels, European Committee for Standardization (CEN), 2006.
[52] F. Zhou, B. Young, Web crippling behaviour of cold-formed duplex stainless steel tubular sections at elevated temperatures, Eng. Struct. 57 (2013) 51–62.
[53] H. Li, B. Young, Design of cold-formed high strength steel tubular sections undergoing web crippling, Thin-Walled Struct. 133 (2018) 192–205.
[54] Z. Fang, K. Roy, H. Liang, P.K.K. Ghosh, A. Mohamed, J. Lim, Numerical simulation and design recommendations for web crippling strength of cold-formed steel channels with web holes under interior-one-flange loading at elevated temperatures, Buildings 11 (12) (2021).
[55] Y. Lian, A. Uzzaman, J. Lim, G. Abdelal, D. Nash, Web crippling behavior of cold-formed steel channel sections with web holes subjected to interior-one-flange loading condition-Part I: experimental and numerical investigation, Thin-Walled Struct. 111 (2017) 103–112.
[56] Y. Lian, A. Uzzaman, J. Lim, G. Abdelal, D. Nash, B. Young, Web crippling behavior of cold-formed steel channel sections with web holes subjected to interior-one-flange loading condition—Part II: parametric study and proposed design equations, Thin-Walled Struct. 114 (2017) 92–106.
[57] F. Arrais, N. Lopes, P. Vila Real, Fire behaviour and resistance of cold-formed steel beams with sigma cross-sections, J. Struct. Fire Eng. 12 (4) (2021) 446–470.
[58] European Committee for Standardization (CEN), NF EN 1993-1-2: calcul des structures en acier – annexe Nationale ′a la NF EN 1993-1-2: calcul du comportment au feu, in: *Eurocode 3*, Belgium, European Committee for Standardization (CEN), 2007.
[59] Y. Cai, L. Wang, F. Zhou, Lean duplex stainless steel tubular sections undergoing web crippling at elevated temperatures, J. Constr. Steel Res. 182 (2021).
[60] Y. Cai, F. Zhou, L. Wang, Y. B, Design of lean duplex stainless steel tubular sections subjected to concentrated end bearing loads at elevated temperatures, Thin-Walled Struct. 160 (2021).
[61] A. Kumar, K. Roy, A. Uzzaman, J. Lim, Finite element Analysis of unfastened cold-formed steel channel sections under end-two flange loading at elevated tempereatures, Advanced Steel Construction 17 (3) (2021) 231–242.
[62] A. Uzzaman, J. Lim, D. Nash, J. Rhodes, B. Young, Cold-formed steel sections with web openings subjected to web crippling under two-flange loading conditions - Part I: tests and Finite element analysis, Thin-Walled Struct. 56 (2012) 38–48.

[63] H.-T. Li, Y. B, Cold-formed high strength steel SHS and RHS beams at elevated temperatures, J. Constr. Steel Res. 158 (2019) 475–485.
[64] European Committee for Standardization (CEN), EN 1993-1-1:2005+A1: design of steel structures – Part 1-1: general rules and rules for buildings, in: *Eurocode 3*, Brussels, European Committee for Standardization (CEN), 2014.
[65] J.-L. Ma, T.-M. Chan, B. Young, Design of cold-formed high strength steel tubular beams, Eng. Struct. 151 (2017) 432–443.
[66] Y. Huang, B. Young, Structural performance of cold-formed lean duplex stainless steel beams at elevated temperatures, Thin-Walled Struct. 120 (2018) 20–27.
[67] European Committee for Standardization (CEN), Env 1993-1-4: design of steel structures – Part 1.4: general rules – supplementary rules for stainless steels, in: *Eurocode 3*, Brussels, European Committee for Standardization (CEN), 2006.
[68] L. Gardner, M. Theofanous, Discrete and continuous treatment of local buckling in stainless steel elements, J. Constr. Steel Res. 64 (11) (2008) 1207–1216.
[69] M. Alabi-Bello, Y. Wang, M. Su, Direct strength method for cold-formed steel beams with non-uniform temperatures, Proc. Inst. Civ. Eng.: Structures and Buildings 174 (9) (2021) 773–790.
[70] G.B.G. Ananthi, K. Roy, J. Lim, Behaviour and Strength of Back-To-Back Built-Up Cold-Formed Steel Unequal Angle Sections with Intermediate Stiffeners under Axial Compression, Steel and Composite Structures, 2022.
[71] M. Naser, N. Degtyareva, Temperature-induced instability in cold-formed steel beams with slotted webs subject to shear, Thin-Walled Struct. 136 (2019) 333–352.
[72] M. Peiris, M. Mahendran, Numerical modelling of LSF walls under combined compression and bending actions and fire conditions, Thin-Walled Struct. 182 (2023).
[73] P. Samiee, S. Esmaeili Niari, E. Ghandi, Thermal and structural behavior of cold-formed steel frame wall under fire condition, Eng. Struct. 252 (2022).
[74] W. Chen, J. Ye, Simplified calculation model for load-bearing cold-formed steel composite walls under fire conditions, Adv. Struct. Eng. 23 (8) (2020) 1683–1701.
[75] A. Ariyanayagam, M. Mahendran, Fire performance of load bearing LSF wall systems made of low strength steel studs, Thin-Walled Struct. 130 (2018) 487–504.
[76] D. Perera, K. Pologanathan, M. Gillie, P. Gatheeshgar, P. Sherlock, I. Upasiri, H. Rajanayagam, Novel conventional and modular LSF wall panels with improved fire performance, J. Build. Eng. 46 (2022).
[77] T. Abeysiriwardena, M. Mahendran, Numerical modelling and fire testing of gypsumplasterboard sheathed cold-formed walls, Thin-Walled Struct. 180 (2022).
[78] Y. Tao, M. Mahendran, A. Ariyanayagam, Numerical study of LSF walls made of cold-formed steel hollow section studs in fire, Thin-Walled Struct. 167 (2021).
[79] E. Steau, M. Mahendran, Thermal modelling of LSF floor-ceiling systems with varying configurations, Fire Saf. J. 118 (2020).
[80] M. Rokilan, M. Mahendran, Design of cold-formed steel wall studs subject to non-uniform elevated temperature distributions, Thin-Walled Struct. 171 (2022).
[81] D. Perera, I. Upasiri, K. Pologanathan, K. O'Grady, B. Nagaratnam, E. Kanthasamy, H. Rajanayagam, Numerical investigation on fire performance of LSF and steel modular floor panels, Buildings 12 (2022).
[82] P. Gatheeshgar, K. Pologanathan, J. Thamboo, K. Roy, B. Rossi, T. Molkens, D. Perera, S. Navaratnam, On the fire behaviour of modular floors designed with optimised cold-formed steel joists, Structures 30 (2021).
[83] X. Yan, T. Gernay, Structural fire design of load-bearing cold-formed steel assemblies from a prototype metal building, Structures 41 (2022) 1266–1277.
[84] Y. Xia, X. Yan, T. Gernay, H. Blum, Elevated temperature and post-fire stress-strain modeling of advanced high-strength cold-formed steel alloys, J. Constr. Steel Res. 190 (2022).
[85] M. Deepak, G.B.G. Ananthi, G. Anupkumar, B. Harini, J. Kumar, Strength enhancements across various parts in intermediate and edge stiffened angle sections due to cold-forming, Mater. Today: Proc. 65 (2022) 1382–1389.
[86] S. Afshan, B. Rossi, L. Gardner, Strength enhancements in cold-formed structural sections — Part I: material testing, J. Constr. Steel Res. 83 (2013) 177–188.
[87] Standards Australia, Australian Standards/New Zealand Standards (AS/NZS) 4100: Steel Structures, Standards Australia, Sydney, Australia, 1998.
[88] British Standards (BS), Structural use of steel work in buildings - Part 8: code of practice for fire restraint design, in: British Standards (BS) 5950-8, London, U. K, 2003.
[89] Bureau of Indian Standards, General construction in steel - code of practice, in: Indian Standards (IS) 800, Bureau of Indian Standards, New Delhi, 2007.
[90] W. Kumar, U. Sharma, P. Pathak, Mechanical properties of low-alloyed YSt-355-FR (0.126%Mo) cold-formed steel tube at elevated temperatures, J. Constr. Steel Res. 192 (2022).
[91] Z. Liang, W. Wang, Z. Wang, Effect of cold-form and tensile strain rate on mechanical properties of Q345 steel at elevated temperatures, J. Constr. Steel Res. 191 (2022).
[92] L. Pieper, M. Mahendran, Mechanical properties of cold-formed steel cladding profiles at elevated temperatures, Thin-Walled Struct. 164 (2021).
[93] X. Yan, Y. Xia, H. Blum, T. Gernay, Elevated temperature material properties of advanced high strength steel alloys, J. Constr. Steel Res. 174 (2020).
[94] W. Chen, K. Liu, J. Ye, J. Jiang, X. C, L. Jin, M. Zhang, High-temperature steady-state experiments on G550 cold-formed steel during heating and cooling stages, Thin-Walled Struct. 151 (2020).
[95] M. Rokilan, M. Mahendran, Elevated temperature mechanical properties of cold-rolled steel sheets and cold-formed steel sections, J. Constr. Steel Res. 167 (2020).
[96] T. Singh, S. K.D, Mechanical properties of YSt-310 cold-formed steel hollow sections at elevated temperatures, J. Constr. Steel Res. 158 (2019) 53–70.
[97] H.-T. Li, B. Young, Material properties of cold-formed high strength steel at elevated temperatures, Thin-Walled Struct. 115 (2017) 289–299.
[98] J. Chen, B. Young, Design of high strength steel columns at elevated temperatures, J. Constr. Steel Res. 64 (6) (2008) 689–703.
[99] J. Yang, W. Wang, Y. Shi, L. Xu, Experimental study on fire resistance of cold-formed steel built-up box columns, Thin-Walled Struct 147 (2020).
[100] L. Pieper, M. Mahendran, Pull-through failure of crest-fixed steel claddings under combined wind and bushfire condition, Thin-Walled Struct. 173 (2022).
[101] K. Liu, W. Chen, J. Ye, J. Jiang, W. Chen, B. Liu, X. C, Experimental investigation on the creep behavior of G550 cold-formed steel at elevated temperatures, Structures 31 (2021) 49–56.
[102] E. Steau, M. Mahendran, K. Pologanathan, Elevated temperature thermal properties of carbon steels used in cold-formed light gauge steel frame systems, J. Build. Eng. 28 (2020).
[103] K. Roy, L.J.H. Lau, P. Yong, G. Clifton, R. Johnston, A. Wrzesien, C. Mei, Collapse behaviour of a fire engineering designed single-storey cold- formed steel building in severe fires, Thin-Walled Struct. 142 (2019) 340–357.
[104] S. Vy, M. Mahendran, Screwed connections in built-up cold-formed steel members at ambient and elevated temperatures, J. Constr. Steel Res. 192 (2022).
[105] American Iron and Steel Institute (AISI), North American Specification for Cold-Formed Steel Structural Framing (AISI S240-15), American Iron and Steel Institute (AISI), Washington, D.C., 2015.
[106] W. Chen, J. Ye, M. Zhao, Steady- and transient-state response of cold-formed steel-to-steel screwed connections at elevated temperatures, J. Constr. Steel Res. 143 (2018) 131–147.
[107] J. Yang, X. Zhou, W. Wang, L. Xu, Y. Shi, Fire resistance of box-shape cold-formed steel built-up columns failing in global buckling: test, simulation and design, Thin-Walled Struct. 183 (2023).
[108] G.B.G. Ananthi, K. Roy, J. Lim, Experimental and Numerical Study of an Innovative 4-channels Cold-Formed Steel Built-Up Column under Axial Compression, Steel and Composite Structures, 2022.
[109] Y. Cai, B. Young, Effects of end distance on thin sheet steel single shear bolted connections at elevated temperatures, Thin-Walled Struct. 148 (2020).
[110] Y. Cai, B. Young, Fire resistance of stainless steel single shear bolted connections, Thin-Walled Struct. 130 (2018) 332–346.
[111] J. Batista Abreu, L.J. Vieira, T. Gernay, B. Schafer, Cold-formed steel sheathing connections at elevated temperature, Fire Saf. J. 123 (2021).
[112] M. Rokilan, M. Mahendran, Design of cold-formed steel columns subject to local buckling at elevated temperatures, J. Constr. Steel Res. 179 (2021).
[113] M. Rokilan, M. Mahendran, Effects of nonlinear elevated temperature stress-strain characteristics on the global buckling capacities of cold-formed steel columns, Thin-Walled Struct. 160 (2021).
[114] J. Pancheti, M. Mahendran, Fire resistance of external light gauge steel framed walls with brick veneer cladding, Thin-Walled Struct. 182 (2023).

[115] W. Chen, K. Liu, J. Ye, J. Jiang, Fire performance of superabsorbent polymers protecting cold-formed steel walls with high load ratios, Thin-Walled Struct. 181 (2022).
[116] E. Steau, M. Mahendran, Elevated temperature thermal properties of fire protective boards and insulation materials for light steel frame systems, J. Build. Eng. 43 (2021).
[117] W. Chen, J. Ye, X. Li, Thermal behavior of gypsum-sheathed cold-formed steel composite assemblies under fire conditions, J. Constr. Steel Res. 149 (2018) 165–179.
[118] Z. Nie, Y. Li, Y. Wang, Mechanical properties of steels for cold-formed steel structures at elevated temperatures, Adv. Civ. Eng. 2020 (2020) 1–18.
[119] K. Ye, F. Ozaki, Post-fire mechanical properties and buckling strength of cold-formed steel hollow section columns, Journal of Constructional Steel 184 (2021).
[120] M. Deepak, Ananthi G.B.G., Buckling capacities of double-T-box girders- A numerical approach, Structures 34 (2021) 4574–4595.